Straining the root on and off triggers local calcium signaling

Vassanti Audemar, Yannick Guerringue, Joni Frederick, Pauline Vinet, Isaty Melogno, Avin Babataheri, Valérie Legué, Sébastien Thomine, Jean-Marie Frachisse

Straining the root on and off triggers local calcium signaling

Vassanti Audemar, Yannick Guerringue, Joni Frederick, Pauline Vinet, Isaty Melogno, Avin Babataheri, Valérie Legué, Sébastien Thomine*, Jean-Marie Frachisse*

Vassanti Audemar, Yannick Guerringue, Isaty Melogno, Pauline Vinet, Sébastien Thomine, Jean-Marie Frachisse : Université Paris-Saclay, CEA, CNRS, Institute for Integrative Biology of the Cell (I2BC), 91198, Gif-sur-Yvette, France.

Valérie Legué : Université Clermont Auvergne, INRAe, PIAF, F-63000 Clermont-Ferrand, France

Joni Frederick, Avin Babataheri : Laboratoire d'Hydrodynamique LadHyX, CNRS, École polytechnique, Institut Polytechnique de Paris, 91120 Palaiseau, France

(*) S. Thomine and J-M Frachisse are Corresponding authors

Classification: Research article, Plant Biology

Keywords: root, mechanotransduction, microfluidics, Arabidopsis, calcium signaling

Abstract

A fundamental function of an organ is the ability to perceive mechanical cues. Yet, how this is accomplished is not fully understood, particularly in plant roots. In plants, the majority of studies dealing with the effects of mechanical stress investigated the aerial parts. However, in natural conditions roots are also subjected to mechanical cues, for example when the root encounters a hard obstacle during its growth or when the soil settles. To investigate root cellular responses to root compression, we developed a microfluidic system associated with a microvalve allowing the delivery of controlled and reproducible mechanical stimulations to the root. In this study, on plant expressing the R-GECO1-mTurquoise calcium reporter, we addressed the root cell deformation and calcium increase induced by the mechanical stimulation. Lateral pressure applied on the root induced a moderate elastic deformation of root cortical cells and elicited a multicomponent calcium signal at the onset of the pressure pulse, followed by a second one at the release of the pressure. This indicates that straining rather than stressing of tissues is relevant to trigger the calcium signal. Although the intensity of the calcium response increases with the pressure applied, successive pressure stimuli led to a remarkable attenuation of the calcium signal. The calcium elevation was restricted to the tissue under pressure and did not propagate. Strain sensing, spatial restriction and habituation to repetitive stimulation represent the fundamental properties of root signaling in response to local mechanical stimulation. These data linking mechanical properties of root cells to calcium elevation contribute to elucidating the pathway allowing the root to adapt to the mechanical cues generated by the soil.

Introduction

Plants are anchored to the ground by their roots. They need to sense environmental cues to adapt to external conditions. Among these cues are external forces like gravity, soil resistance, wind or touch by animals. In contrast to aerial organs, roots experience high mechanical stresses due to pressure exerted by the soil. In order to penetrate the soil and to overcome physical obstacles, the root generates an axial force. At the same time, during its progression, lateral confinement along the radial

axis increases, generating lateral forces [1], [2]. Soils scientists often consider “soil structure” as the spatial arrangement of the different components and properties of soil [3]. A typical volume of surface soil includes about 50% solids, mostly soil particles (45%), and organic matter (generally < 5%) and about 50% pore space [1]. Therefore, during their growth, roots progress in a heterogeneous network crossing empty cavities and substrates of various stiffness. The thrust force (or pushing force) exerted by the growing part of the root has to overcome the soil resistance as well as the lateral friction with the soil. The friction involved in the balance of forces is the one acting on the flanks of the root along the elongation and meristematic zones [1]. A local lateral confinement around the radial axis is a scenario that the root can encounter. Such a stress occurs for example when the soil settles or upon radial growth of the root squeezed between two hard fixed soil particles. To our knowledge, the characteristics of physical and biological responses locally elicited by such a compressive, non-wounding stimulation, have so far not been investigated.

Calcium is one of the most important ions for signal transduction. Free cytosolic calcium concentration increases in response to many signals. The duration, amplitude, frequency and spatial distribution of the calcium elevation is controlled by calcium channels, transporters and pumps localized in the cell membranes [4]. The spatio-temporal pattern of cytosolic calcium elevation was shown to encode information allowing specific responses to diverse cues that involve cytosolic calcium as a second messenger [5], [6]. Notably, it has been shown that calcium is involved in signal transduction of touch [7]. Rise and propagation of a calcium signal in the case of Venus flytrap induces the closing of the leaf [8]. *Arabidopsis thaliana* also displays a calcium signal after local stimulation of a root cell with the tip of a micropipette [7]. Macromolecules involved in the control of cell wall integrity embedded in the membrane or in the cell wall could be recruited for transduction of a mechanical stress into biological responses including calcium variations [9]. For example, FERONIA (FER), a transmembrane protein was shown to be involved in root mechanoperception [10]. Moreover the *fer* mutant shows an alteration of the calcium signal elicited by touching or bending the root [10]. The plasma membrane is also subjected to mechanical stress due to tensile or compressive forces and variation of osmotic pressure [11]. Calcium permeable mechanosensitive channels at the plasma membrane are good candidates to mediate cytosolic calcium elevations in response to membrane deformation induced by touch or cell compression. Thus far, five families of mechanosensitive ion channels MSL, Piezo, OSCA, MCA and TPK have been identified at the molecular level and electrophysiologically characterized in *Arabidopsis* [12]. An additional mechanosensitive channel called RMA (Rapid Mechanically Activated) was characterized at the plasma membrane of Arabidopsis, but its molecular identity is not yet determined [13]. All these mechanosensitive channels except for MSL are calcium permeable but also permeable for other divalent and monovalent cations. With rapid activation and inactivation, Osca, Piezo and RMA share common kinetic properties [14].

Here we address the following questions: Could a compression mimicking the lateral confinement generated by the soil pressure deform the root? What are the specific properties of the calcium signal elicited by such strain? We developed a microfluidic device enabling us to apply a controlled mechanical lateral stress on the root to address these questions. The microfluidic device allows imaging of plant roots with a microscope for long durations with a high spatio-temporal resolution. We used confocal microscopy to image and quantify cell deformation and epifluorescence microscopy combined with a fluorescent cytosolic calcium reporter to characterize the calcium signal induced by lateral strain on *Arabidopsis thaliana* roots.

Materials and Methods

Microfluidic device manufacturing

The polydimethylsiloxane (PDMS) devices were made using standard dry film and soft lithographic procedures based on the method by Dangla *et al*. (2013) [15]. To produce moulds for the root growth

channels, two layers of Eternal Laminar E8020 dry photoresist film of thickness 49± 2 µm were successively deposited on a glass slide by lamination at 100 °C to reach a desired channel height of ~100 µm. The film was UV exposed through a photomask designed using CleWin5, to produce straight channels with height, width and length of ~90 µm, 600 µm and 2 cm, respectively.

The channels were replicated from the master moulds in degassed PDMS with a 1 to 10 ratio of curing agent to bulk material (SYLGARD 184 elastomer and curing agent, Dow Corning), cured at 70 °C for 2 hours to obtain the device pieces. PDMS blocks serving as root growth channels were replicated with a strictly controlled height, so that once bonded to a glass coverslip, the top part of the channel leaves a PDMS membrane with a thickness of 250 or 460 µm which serves as a deformable push-down valve. PDMS blocks serving as pressure channels sitting above the plant growth channels were made using the same procedure, and with a thickness of 4 mm +/- 1 mm. A spin coater (Model WS-650MZ-23NPPB, Laurell) was used to obtain a thin layer of PDMS to coat coverslips . Several devices with different membrane thicknesses were produced by varying the time or rotational speed of the spin coating process. Membrane thicknesses were measured by profilometry (ProFilm3D, Filmetrix) (Supplementary Fig. 1). PDMS pieces were peeled off the molds, and pierced with 1mm holes to create liquid and gas inlets/outlets. Additional holes were punched at a 45° angle to serve as the entry path connecting the root with the root growth channels before sealing by plasma treatment (Harrick Plasma, Plasma Cleaner PDC-002-CE) together and to a glass coverslip covered with a thin (37 +/- 2 µm) PDMS layer.

Plant material and growth conditions

Seeds of Arabidopsis thaliana (Col-0 ecotype) constitutively expressing RGECO1-mTurquoise under the UBQ10 promoter [16] were sterilized in ethanol 70% and SDS 0.05% for 5 min, rinsed with ethanol 96% for 5 min and dried at room temperature. Then, the seeds were sown on conical cylinders produced by cutting micropipette tips containing Hoagland medium (1.5 mM $Ca(NO_2)_2$, 0.28 mM KH_2PO_4, 0.75 mM $MgSO_4$, 1.25 mM KNO_3, 0.5 µM $CuSO_4$, 1 µM $ZnSO_4$, 5 µM $MnSO_4$, 25 µM H_3BO_3, 0.1 µM Na_2MoO_4, 50 µM KCl, 3 mM MES, 10 µM Fe-HBED, pH 5.7) with 1% phyto-agar, they were inserted into Petri dishes filled with the same medium [17]. After 3 days of stratification at 4°C in the dark, the seeds were incubated in 16h light/ 8h dark at 22°C during 3 days in a culture chamber. After the primary root reached the bottom of the cone, they were transferred from the Petri dish to the microfluidic device (Fig. 1b) and kept under the same temperature and light conditions. Root growth was conducted into the root channel filled with liquid Hoagland medium. During the growth, the device was tilted with an angle > 45° to allow the root to grow gravitropically. Root channels were connected by tubing to syringes filled with liquid Hoagland medium, and the channel medium was refreshed with a flow rate of 1 µL/min using a syringe pump.

Acquisition protocol

When root growth had extended passed the deformable membrane portion of the PDMS device, i.e. 6 or 7 days after transfer to the incubation chamber, microscopy experiments were launched. The root channel was connected by tubing to syringes filled with liquid Hoagland medium and connected to a syringe pump (WPI, AL-1000) enabling control of the flow rate. The pressure channels were connected by tubing to a pressure box (Fluigent, MFCS-EX) that allows injection of an air flow at a fixed pressure into these channels. The PDMS device was secured in a 3D printed sample holder fitted with a Perspex lid and designed to fit in a standard 96-well plate sample holder.

Cross-sectional views of the microfluidic channels and cross sections of the roots were acquired with a Leica SP8 inverted microscope equipped with, a white light laser (470 to 670 nm), and two GaAsP Hybrid detectors (Hamamatsu). For cross sections of the channels, fluorescein solutions at 10 µM were imaged with a 10x PLAN APO dry objective (Leica) at λex = 488 nm and λem = 501-609 nm. For cross section of the roots, cell walls were labelled with propidium iodide (5 µg/mL) and imaged using a 20x PLAN APO multi-immersion objective (Leica), with λexc = 488 nm and λem = 551-651 nm. A Leica DMI

6000 inverted microscope equipped with an excitation lamp (PE-4000 LEDs, CoolLed), a quad band dichroic mirror (Chroma) and black and white camera (CoolSNAP HQ² CCD, Photometrics) was used to image intracellular calcium. R-GECO1-mTurquoise fluorescent lines were imaged using a 5x dry objective with λexc = 580 nm and λem = 600-700 nm for R-GECO1 and λexc = 470 nm and λem = 490-520 nm for mTurquoise.

Image acquisition frequency for short stimulation (30 sec) was 1 frame every 15 second and for long stimulation (20 min) 1 frame every 6 sec.

Image processing and data analysis

Image processing and analysis was performed using Matlab. Length variations of cells along Oy and Oz axis (Fig. 3) were measured on cross-sectional views of wild type roots stained with propidium iodide. Image analysis was conducted following these steps: the background was subtracted and a segmentation was performed to delimit cell boundaries. Maximal length of each cell in the horizontal and vertical dimension was measured before and during the pressure stimulation using bounding box (Supplementary Fig. 2). Calcium signal variation measurements were performed as follow: for each time point, the background was subtracted and a binary image was generated. The root axis was extracted and segments of 100 µm perpendicular and centered around this axis were distributed at 50 pixels intervals (Supplementary Fig. 2d). Mean values of the ratio between R-GECO1 images and mTurquoise images were calculated for each segment along the root and reported in heat maps representing calcium concentration variations along the root axis over time.

Results

Setting up a micromechanical system for delivering lateral pressure

In order to apply a controlled lateral compression to the root, we have developed a microfluidic device combining a rootchip [17] with a pressure system inspired by a micromechanical push-up valve [18]. The device was fabricated in PDMS which has been shown to be biocompatible with *Arabidopsis thaliana* [19]. Three layers of PDMS were sealed together, enabling the formation of channels: the pressure channels containing air sit on top of the root channels in which the root is growing, while the whole PDMS device is bound to a glass coverslip covered in a thin PDMS film to enable the visualization of the root with an inverted microscope (Fig. 1a).

The perpendicular layering of the root channel and pressure channels defines a square PDMS membrane (Fig. 1b) with an active area of 600 µm by 600 µm (Fig. 1c). The PDMS deformability and the specific dimensions, especially the thickness/side length aspect ratio, allow the membrane to deflect downward into the root channel when a sufficiently high pressure is injected into the pressure channel. In our device, two of these micromechanical push-down valves are distributed 2 mm apart over the root channel (Fig. 1b), and each pressure channel can be controlled individually.

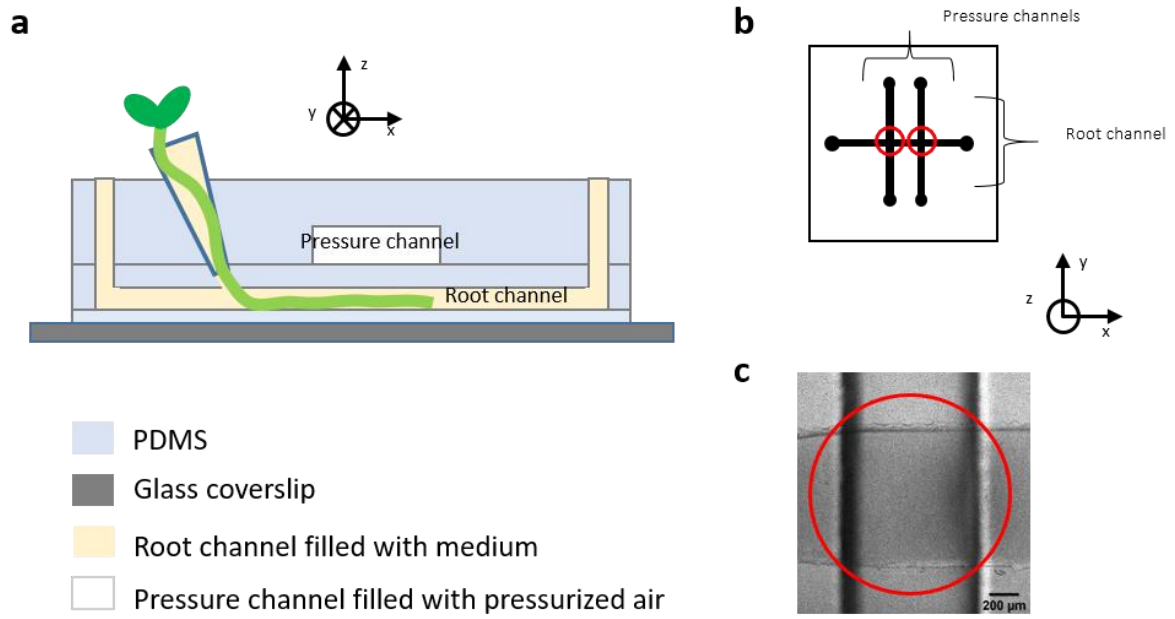

Figure 1: Microfluidic device equipped with a pneumatic valve. a) Schematic side view of the microfluidic device containing the plant root channel and pressure channel separated by a flexible push-down PDMS valve. b) Schematic top view of the two mechanical push-down valves at the intersections of the root channel and the pressure channels. c) Top view of a mechanical push-down valve imaged in bright field (Leica DMI 6000, 5x objective). Valves areas have been circled in red.

We compared the deflection, called **d**, of the push-down membrane of microfluidic devices with two different membrane thicknesses: 460 +/- 57 µm and 250 +/-31 µm (as annotated in figure 2). The 250 µm PDMS membrane exhibits a greater deformability for the same pressure (shown in cross-sectional views of the root channels without root perfused with a solution of fluorescein at 10 µM with a constant flow rate of 8 µL/min; supplementary Fig. 3). A compromise had to be made for the PDMS membrane thickness to be thin enough to increase the deformability and enable a good transfer of pressure from the pressure channel to the root, but thick enough to avoid damage during the device manufacturing process. In further experiments, the PDMS membrane thickness was fixed at 250 µm.

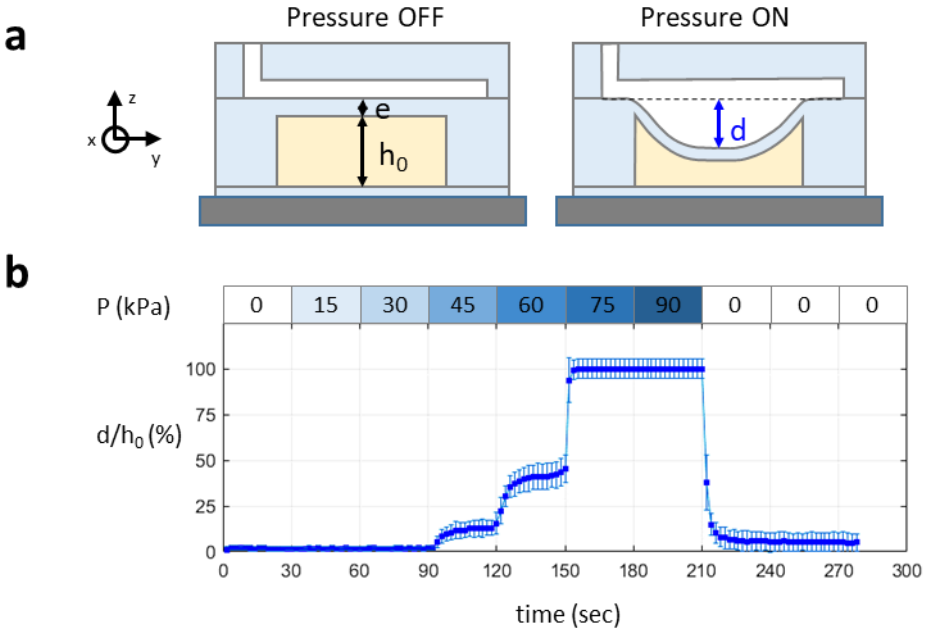

Figure 2: Relationship between membrane deformation and pressure in the air channel. a) Schematic cross section of the pneumatic valve with and without pressure: **e** is the thickness of the PDMS membrane separating the pressure channel (white) and the root channel (yellow), $\mathbf{h_0}$ is the height of the root channel before pressure and is equal to 90 µm, **d** is the maximum distance between the center of the valve membrane at rest and in its deformed state when pressure is applied. b) Variations of **d** reported as a percentage of h_0, the maximal deformation of a 250 µm thick PDMS membrane with applied pressure. Measurements were repeated 3 times on 4 different valves. Squares correspond to the mean values of all measurements and error bars correspond to standard deviations.

We measured the deflection of the 250 µm PDMS membrane as a function of the pressure increasing by steps of 15 kPa every 30 seconds. The percentage of the deflection length, **d**, normalized by the thickness of the channel $\mathbf{h_0}$ is presented in figure 2b. Deformation is triggered with pressure from 45 kPa and continuously increases with pressure, until the valve membrane reaches the bottom of the channel ($d = h_0$) at 75 kPa. This system without root has a typical time to reach the equilibrium state of around 10s. Upon release of the pressure, the membrane returns to its approximate initial position. The number of stimulations on the same valve does not impact its ability to deform. The short standard deviations indicate that the system is reliable and does not experience damage with repeated stimulations.

Lateral pressure induces elastic deformation of the root cells

We assessed the mechanical response to a pressure of 90 kPa applied through the deformable PDMS membrane (also called valve) on primary roots of 7 days old seedlings in the maturation zone (1-5 mm from the apex). Confocal images of root cross sections were used to measure the deformation of the root in the Oyz dimension. Cell walls were stained with propidium iodide to visualize cell shape. A segmentation analysis was performed to identify the outlines of cells (Supplementary figure 2a, Supplementary video 1). We measured the length of the cells, L_y and L_z projected on the Oy and Oz axes, transversal and longitudinal to the applied force respectively. D_y and D_z are the corresponding relative length variations defined by $D_y = (L_y - L_{y0})/L_{y0}$ and $D_z = (L_z - L_{z0})/L_{z0}$, with L_{y0} and L_{z0} the projected length on Oy and Oz axes before the application of the pressure. Cells located in the upper part of the image were out of the working distance of the objective and therefore could not be segmented. Cell walls located in the central cylinder were not stained by propidium iodide and therefore were not segmented, thus we considered the central cylinder as one object.

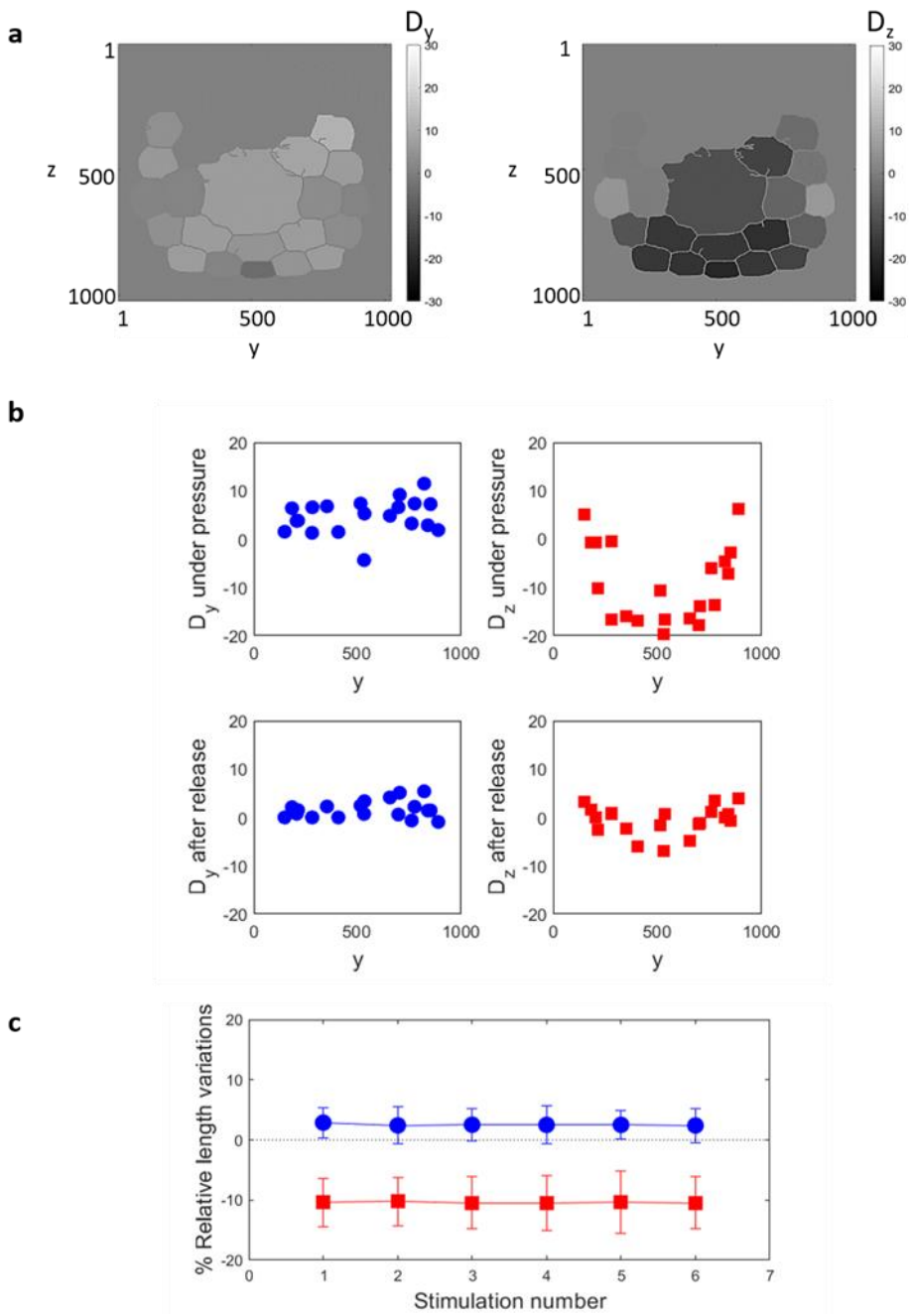

Figure 3: Transversal and longitudinal relative length variations D_y and D_z: a) Representation of the segmented cells of one representative root under a pressure stimulation of 90 kPa. Each cell was colored with a grey level corresponding to the percentages D_y on the left and D_z on the right. b) Percentage D_y and D_z of one representative root during the first stimulation and after the release in function of the transversal dimension Oy. c) Percentages D_y and D_z averaged over all the segmented cells of a root stimulated 6 times every 5 min with a pressure of 90 kPa during 1 min. The plain symbols represent the mean value of 19 different roots and the error bars represent the standard deviation associated. For b) and c), the blue circles and red squares correspond to D_y and D_z respectively.

Under pressure, D_y and D_z show a heterogeneous repartition between the cells of the cross-section due to the geometry of the applied force and the connectivity between the cells (figure 3a), resulting in a complex tension field. For example, the cells located on the lateral sides experience a positive variation in length D_z, indicating an elongation instead of the compression observed among the other cells. Figure 3b shows the repartition of D_y and D_z along the transversal axis O_y for the root under pressure and after release. The distribution of D_y is roughly constant along the O_y direction whereas D_z

experiences a symmetrical distribution with respect to the midline of the root in the Oz direction, with the largest relative length variations corresponding to the cells close to the midline (fig. 3a). After release of the pressure, the initial cell shapes were recovered with values of D_y and D_z close to 0 %, showing a reversible deformation process.

Six repeated stimulations every 5 minutes have been performed on roots with a pressure of 90 kPa during 60 seconds, on 19 roots in the maturation zone (1-5 mm from the apex). The average percentages of D_y and D_z over all the cells per root were calculated. No correlation was revealed between the average percentage of length variations and the position along the main axis. Under a stimulus of 90 kPa, D_z was around 10 % and D_y around 4%. After 6 stimulations, no significant difference in relative length variation was found as shown in figure 3c.

Lateral pressure elicits a local elevation of cytosolic calcium concentration

We used the fluorescent ratiometric reporter RGECO1-mTurquoise [16] to monitor variations of cytosolic calcium concentration in root cells. The reporter designed to probe cytosolic Ca^{2+} was constitutively expressed in all tissues of *Arabidopsis thaliana*, and we measured the ratio R between the R-GECO1 fluorescent signal, sensitive to the calcium concentration, and the mTurquoise fluorescent signal, used as a control of the expression of the reporter (Fig. 4a and Supplementary figure 4). The mean ratio on each segment along the root axis (Supplementary figure 2b) was normalized as R / R_0, with R_0 corresponding to the baseline value of R before any stimulation. Each segment value was represented on heat maps in Figure 4b, as a function of the time and the position along the main root axis. This was done for two types of stimulation at 90 kPa: a short stimulation of 30 s, or a long stimulation of 20 min. The projection of the root area was measured before (A_0) and during (A) the pressure. Because of the deformation of the organ, the projected area of the root under pressure is greater than in the absence of pressure. The normalized projected area A / A_0 and the average value of the ratio $\overline{R / R_0}$ were calculated on the portion of the root located under the valve and are represented in Figure 4c with the pressure protocol associated. In either case, the variation of the projected area was around 5% and recovered its initial level after the release of pressure, indicating a small elastic deformation. The recording of the ratio $\overline{R / R_0}$ displayed a multicomponent signal with two distinguishable phases: a rapid and sharp elevation (labeled with an asterisk, Fig.4c) with a maximum occurring at 10 ± 3.7 s after the beginning of the stimulation, followed by a smoother rise and decrease of the signal with a maximum at 100 ± 15.5 s, that recovered its initial value within 15 minutes (Supplementary video 2 and video 3). The acquisition rate adapted to long lasting recording (see Material and Methods) was not sufficient for an adequate resolution of sharp spike. Therefore, the amplitude of the initial fast spike was not quantified. In the case of the long stimulation, a second increase of calcium of lower amplitude was elicited by the release of pressure (Figure 4c and d). The calcium increase was mainly localized between the boundaries of the valve and no clear propagation along the root axis was observed.

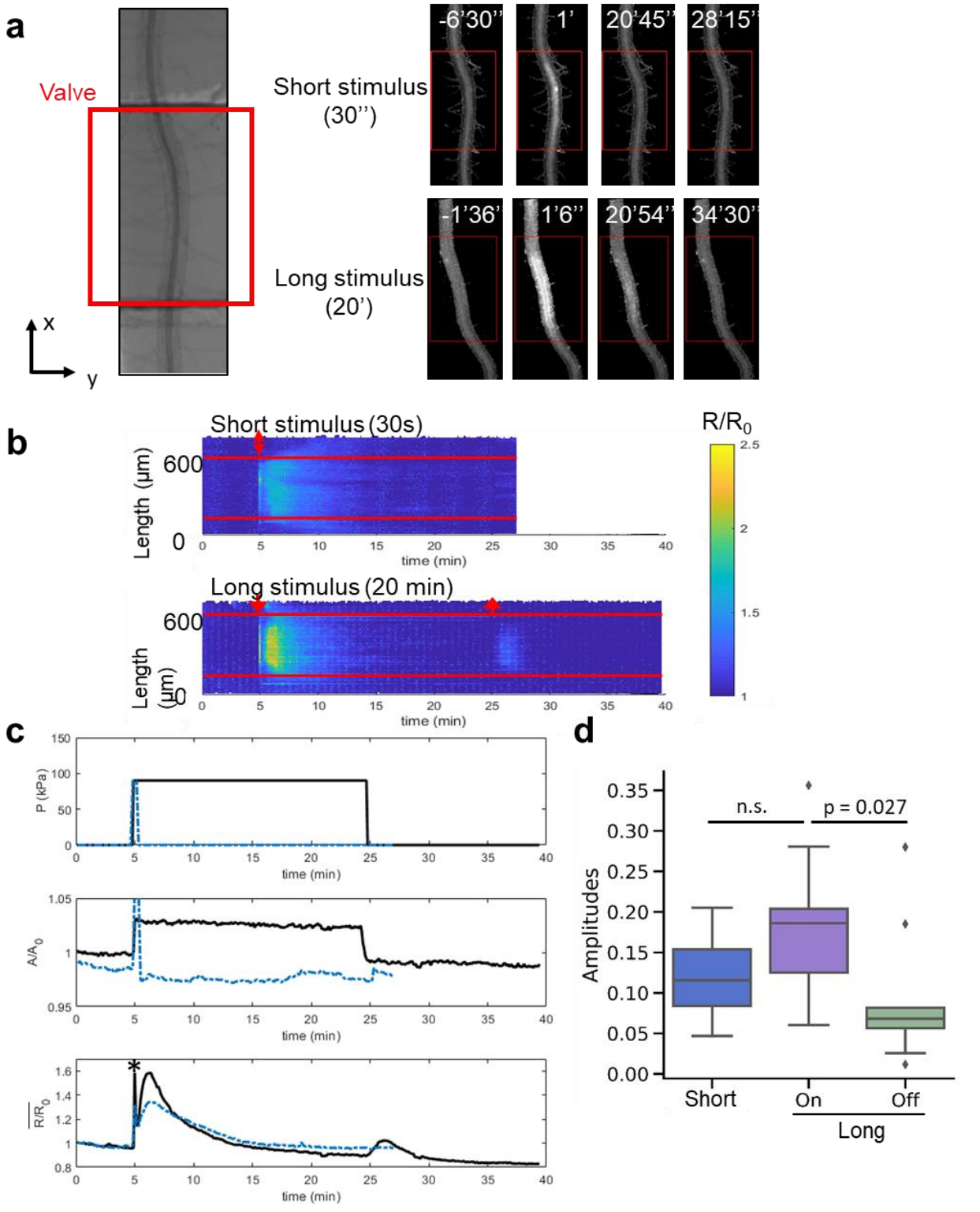

Figure 4: Calcium response, in time and space, to a local short (30 s) and long (20 min) applied pressure of 90 kPa: a) Bright field image (left) of the root under the pneumatic valve. RGECO-mTurquoise fluorescence ratio images (right) of the short and long stimuli, origin of time at the beginning of the pressure application (negative time before the pressure). b) Kymograph showing variations of the mean normalized ratio R/R0 (cf Material and Methods) along the main root x axis during time, represented as heat maps for a 30 s stimulus (top image) and a 20 min stimulus (bottom image). The red lines correspond to the position of the pneumatic valve and the red arrows to the time of stimulation (activation and release). c) Time variations of the pressure stimulation (top), the normalized projected area of the root (middle) and the calcium signal ratio normalized to the value at time

0 (bottom) elicited by a pressure of 90 kPa during 30s (dotted blue line) and 20 min (black line). (*) indicates the calcium spike observed in most of recordings at the onset of the stimulation. The graphs show one representative experiment out of 23 for short and 9 for long stimulation. d) Amplitudes of the calcium variation triggered by a short stimulus (N=23) or by the activation (On) and release (Off) of pressure during a long stimulus (N=9). ANOVA and post-hoc Tukey test indicate a significant difference between the On and Off amplitudes for a 20min stimulus (Tukey pairwise test p-value < 0.05).

The amplitude of the cytosolic calcium concentration increases with increasing pressure intensity

In order to analyse the relationship between the pressure intensity and the amplitude of the cytosolic calcium concentration, we subjected the root to mechanical stimulations of 30 s with an increasing pressure intensity using the pressure protocol presented in Figure 5a (top panel). The normalized area presented in Figure 5a (middle panel) showed an increase corresponding to the increasing pressure. We could also observe the increase of the amplitude of the calcium elevation as represented in figure 5b. However, repetition of the pressure stimulation at 75 kPa (for 2 plants) or further increase to 90 kPa (1 plant) triggered a rise in cytosolic calcium with a lower amplitude (Supplementary figure 5). This indicates that the system is indeed sensitive to the intensity of pressure and suggests that it undergoes attenuation upon repetitive stimulations or at supra-optimal pressures.

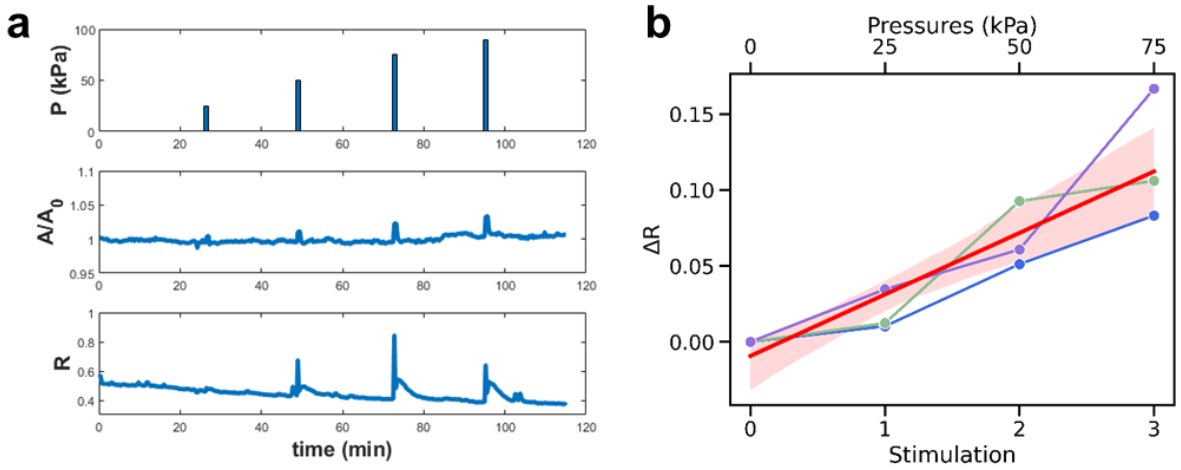

Figure 5: Successive stimulations of 30 s with an increasing pressure: a) pressure (top), normalized area (middle) and calcium signal ratio (bottom) for one representative plant. b) Amplitude of the calcium signal for three successive stimulations of 25, 50, and 75 kPa in three different roots (blue, green, purple). Linear regression in red plotted with the confidence interval (light red band); slope = 0.00162, R2 = 0.90, p-value = 7x10-5 (bottom x-axis: stimulation number; top x-axis: stimulation pressure).

Repeated stimulations lead to attenuation of the calcium elevation

To test whether the decrease of the calcium elevation upon increasing pressure stimulation (Fig. 5) is due to an intrinsic attenuation, we tested the effect of repetitive stimulations of the same amplitude. In Figure 6, we subjected roots to repetitive pressure stimulations of 30 s at 90 kPa every 5 min. The calcium signal in response to the first pressure pulse presented the highest intensity. The amplitude of the second peak was decreased by more than 50% compared to the first one, while the amplitude of following peaks subsequently decreased following each stimulation. These results indicate that the system displays attenuation upon repeated stimulation. To test the effect of the frequency of stimulation, and whether the system recovers from habituation after a longer delay, we imposed 30 second stimulations at different time intervals. In Figure 6b, the time interval between two pulses was increased to 20 min or 60 min. The amplitude of the calcium rise decreased irrespective of the delay

between two stimulations. The rate of decrease between the stimulations was not different at different stimulation frequencies. This indicates that the relevant factor for attenuation is the repetition of the stimulations and not their frequency (time elapsed between two stimulations), and that the calcium dynamics system does not recover after 60 min.

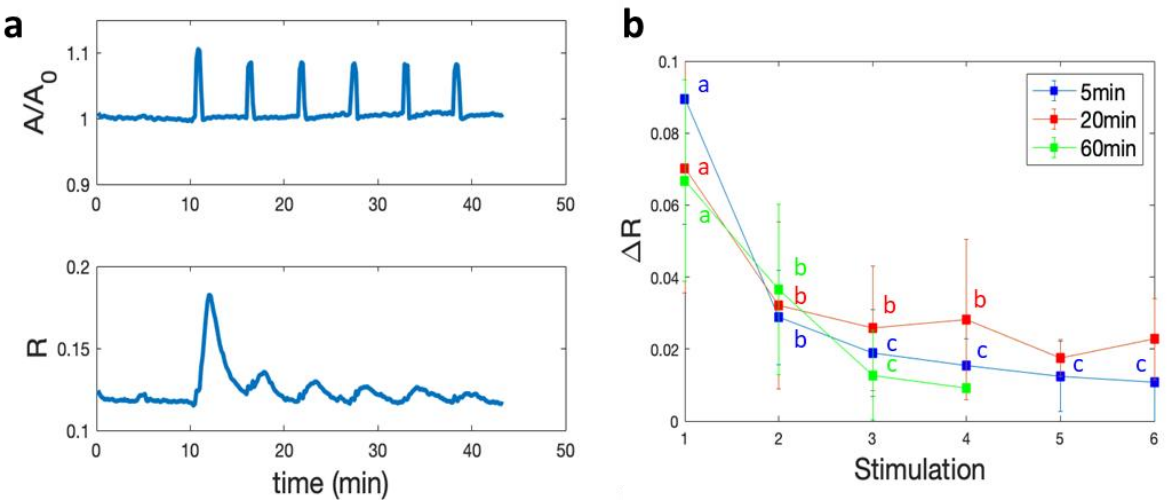

Figure 6: Repeated pressure stimulations lead to a decrease in the amplitude of the calcium signal. a) normalized area variations (top) and calcium signal ratio (bottom) in a representative experiment, b) Maximum amplitude of the calcium ratio peaks for each stimulation of 30 s at 90 kPa every 5 min (blue, n = 6), 20 min (red, n = 5) and 60 min (green n = 4). Significantly different groups (a, b, c) were constituted following a repeated measures ANOVA (p-values of 3x10-10, 1x10-5 and 8x10-4 for 5 min, 20 min and 60 min respectively) and a post-hoc pairwise t-test with a Benjamini/Hochberg FDR correction (corrected p-value <0.05).

Discussion

We designed a microfluidic device allowing reproducible mechanical stimulation of roots. Our experimental design proved to be suitable for investigating root deformation together with calcium variation induced by a mechanical stress. Precise description of the strain generated by a local compression was achieved at the tissue and cellular levels. The analysis of the cytosolic calcium concentration in terms of kinetics, intensity and tissue location allowed us to characterize the Ca^{2+} variation and to link it with the local strain.

This system could be used to monitor a wide range of cellular parameters and events in response to gentle pressure stimulation. For example, the characterization of organelle shape and position upon mechanical stress would bring valuable information. Considering the variety of fluorescent probes now available and the ability to label proteins involved in mechanosensing, our system should allow addressing key questions in mechanotransduction such as, for example, microtubule reorganization and membrane tension variation.

From soil mechanics to microvalve stimulation

Investigation of root biomechanics was initiated by biophysicists considering that root and soil form a continuum [20]. In these studies soil-root interaction is described with macroscopic variables such as the Young's modulus of root tissue, soil penetration stress [21] and quantification of the energy

required to deform the root [22]. In recent approaches, researchers developed experimental systems allowing to record microscopic particle forces and their effect on strain and stress at the tissue and cell scales [20]. In the classification of the root mechanical response based on soil scale heterogeneity, soils containing objects of large size (immovable objects) might be compared with the stimulation applied by the valve [1]. In this situation radial force are locally exerted along the root at the contact point with the object [20]. Kolb et al. (2012)[23] developed an original method of photoelasticity to measure root radial forces. The experimental setup allowed constraining the lateral root growth inside a gap and to measure *in situ* the corresponding force. During chick pea (*Cicer arietinum* L.) root growth, they measured the radial force for a duration of 45 h. The dynamic of the force was in the range of 0 to 5 N from the contact of the disc with the root up to 45 h of recording. Taking into account the contact surface of the disc (of the order of 5 mm^2), the estimation of the average mechanical stresses is 0.30±0.15 MPa (or 300±150 kPa; [23]). In our present study, considering the high elasticity of the valve (S-Fig 3), the entire lateral surface of the root is under contact with the valve membrane. Therefore, we could approximate that the maximal stress delivered is close to the pressure applied in the valve, i.e. 90 kPa for highest stimulation. The stress produced by constraining the lateral root growth of chick pea is of the same order of magnitude than the one we apply on Arabidopsis root. This stress value is of the same order of magnitude as the turgor pressure, which generally varies in a range of 0.1–1MPa (100-1000 kPa) [24], [25]. It should be noted that this range ofpressure provide enough force to destruct hard elements of the soil such as stones or even concrete.

The calcium signature in response to mechanical stress

We observed a calcium signal composed of two components, a fast calcium increase peaking after a few seconds and a slower calcium response lasting a few minutes (Fig. 5 and 7), which are not propagated along the root. Monshausen et al. [7] also showed that both touching the surface of the Arabidopsis root or bending the root elicited a local calcium elevation. In both cases, the cytosolic calcium concentration rapidly increased and then returned to its initial concentration 10 minutes after bending and 60 seconds after touching. Mousavi et al. [26] monitored the calcium response to non-damaging mechanical indentation of the root cap of Arabidopsis. Likewise, increasing the amplitude of the indentations elicited a transient and localized Ca^{2+} signal in the columella and lateral root-cap cells. In addition, they showed that depleting the plant from the mechanosensitive channel PIEZO1 diminished the calcium transient [26]. When bending Arabidopsis root, Shih et al. [10] elicited a biphasic calcium response composed of a short peak followed by a longer wave. The longer wave was attributed to the activation of the Receptor-like Kinase FERONIA. A biphasic calcium response was also elicited by ATP in Arabidopsis roots. Matthus et al. [27] attributed the slow component to the activation of the plasma membrane receptor DORN1/P2K1, while the rapid component was attributed to the mechanical perturbation of the root through the experimental system. The calcium signature elicited by gentle mechanical stimulation is distinct from the signal induced by salt stress or wounding. Local treatment of the root with NaCl triggers Ca^{2+} waves that propagate through the plant at rates of up to ∼400 $\mu m.s^{-1}$ [28]. Calcium signaling induced by wounding the aerial parts or the root elicited a propagated wave of calcium delivering an information to remote organs [29].

Compared to previous studies, our microfluidic set-up revealed new features of the calcium response: (i) a local calcium elevation is observed upon increase but also upon release of the pressure, (ii) the intensity of the calcium response increases with the pressure applied and (iii) successive pressure stimuli lead to attenuation of the calcium signal.

Attenuation

We have shown two important properties of the calcium signal, (1) after a rapid raise of calcium the signal slowly recovers its initial level after 10 minutes whether the pressure is sustained or not, and (2)

the repetition of stimulations leads to a decrease in the amplitude of the calcium signal. Rapid increase in calcium, in response to various physical stimuli such as cold shock, osmotic shock or touch has been reported in plants [7], [30], [31]. With these three stimuli, when sustained, the calcium concentration rapidly decreases within a few tens of seconds to a few minutes after the initial peak. In *Arabidopsis* and tobacco plantlets, the cold-induced increase in calcium is attributed to an influx of Ca^{2+} from the extracellular medium relayed by an intracellular store. Then, recovery would be due to ER and vacuolar uptake of calcium from the cytosol [30]. In *Arabidopsis* guard cells, performing successive depolarizing hyperosmotic KCl shocks, the authors showed that cytosolic Ca^{2+} concentration controls stomatal closure by two mechanisms, a short term `calcium-reactive' closure and a long-term `calcium programmed' steady-state closure [31]. Furthermore, similar to our results, an attenuation of the calcium signal is noticed upon repetition of the 5 minute KCl shocks every 10 minutes.

As part of an integrative approach, Martin *et al.* [32] have addressed the effect of wind stress on plant growth and gene activation by performing multiple stem bendings on young poplars. They observed a decrease of the molecular response to subsequent bending as soon as a second bending was applied. They called this phenomenon desensitization and determined a refractory period of 7 days needed to recover a gene expression activation similar to that observed after a single bending.

The processes of amplification, attenuation and desensitization of the electrical signal have been most investigated in the neural system in the context of the transmission of information. In neurons, the action potential (AP) might fire up to a frequency of 500 Hz. In this system, the transmission of signals via chemical synapses represents a very dynamic process. The synapse, playing a role of relay, is able, in situations of prolonged stimulation, to attenuate the signal [33]. The purpose of such an attenuation would be to process the information and to adapt to an excess of signal, such as mentioned for the auditory system [34]. The shape and the amplitude of the signal can be directly modified by the ion channels generating the AP. For example, in the case of a high stimulation frequency, some channels still being in their relative refractory period, APs will be modified in their shape and/or their frequency [35]. It is also exemplified by Cain et al. [36] who showed that the kinetic properties of several isoforms of T-type calcium channels are closely linked to their contribution to neuronal firing. Mutations of T-type calcium channels could be associated with certain pathophysiological disorders. The examples of attenuation mentioned above operate at different time scales, from milliseconds for APs in a nerve, to minutes in guard cells and roots of *Arabidopsis*, and up to days for poplar gene expression. Nevertheless, in all examples mentioned, attenuation leads to an adaptive response of the cell/organ/organism, and the primary actors of the generation of the signal are likely ion channels.

Strain-stretch hypothesis, its physiological relevance

In the soil, the thrust force (or pushing force) is exerted by the elongating part of the root. This force has to overcome the soil resistance as well as the lateral friction, acting on the flanks of the root [1]. In a heterogeneous soil with fixed obstacles, the elongating and mature zones are subjected to lateral forces while growing in a constriction of the root diameter size [1], [20]. Our study specifically addresses the mature zone that experiences only radial compression. This zone is physiologically relevant in term of root anchorage and also for its ability to exert high force in the constriction zone and thus to weaken the substrate.

Calcium increase is triggered at the onset of pressure and at the release of the pulse of pressure. Similarly, responses to “touch” and “letting go” have been reported for epidermal cells of Arabidopsis and tobacco [37]. In that case, distinct characteristics of the waves elicited by the compressive force and its release suggest different underlying mechanisms for the “touch” and “letting go”. In our

experiments, calcium release corresponds to the time when the maximum of strain variation in the root cells is observed. Indeed, tissue shape variation occurs when strain is applied and released. Although they differ in amplitude, probably due to attenuation, the calcium waves elicited by pressure and release share the same characteristics. This indicates that strain rather than stress triggers calcium signals underpinned by a common mechanism.

In biological materials, stress is not proportional to strain, therefore stress-sensing and strain-sensing mechanisms have different output [38]. For example, in Arabidopsis pavement cells, microtubules, which align in the direction of maximal mechanical stress, are postulated to play a role as a mechanosensor [39]. However, James *et al.* reported that more generally the stimulus for growth sensed by cells is the mechanical strain rather than the stress [40]. Furthermore, in agreement with our finding, Moulia *et al.* showed that the strain-sensing model is better suited than the stress-sensing model to explain the primary and secondary thigmomorphogenetic growth-responses in trees [41].

Several recent studies highlighted the role of calcium in long distance systemic signaling. Calcium signaling induced by wounding the aerial parts or roots elicited a propagating wave of calcium delivering information to remote organs [29]. Here, with gentle local pressure the signal is restricted to the pressurized zone. Only strained tissues display a calcium signal. This signaling path probably indicates that cells have to react and adapt to the local deformation of the root. Thus, when a root is squeezed between hard objects such as stones, lateral tissues are likely pressure-stimulated, inducing a local calcium signal allowing the plant to adapt to this local soil constraint.

What could be the molecular mechanisms underlying the calcium increase?

Although the calcium signature in response to mechanical cues displays common features, the molecular mechanism remain elusive. Not only the number of candidate receptors and channels possibly involved in Ca^{2+} response are numerous, but also calcium sources are diverse. Indeed, many Ca^{2+} reservoirs are present in the cell, notably the vacuole, the endoplasmic reticulum (ER) and other organelles [42], [43]. The kinetic behavior of transient Ca^{2+} signals was modeled at the cell level and proposed to result from four components, two Ca^{2+} permeable channels located at the plasma- and endo-membrane, respectively, and two active Ca^{2+} efflux systems, a plasma membrane-based Ca^{2+} ATPase pump and endomembrane-based Ca^{2+}/H^{+} exchanger [4]. In our case, one can hypothesize that the short peak relies on the activation of mechanosensitive channels, which immediately activate upon membrane tension. The slower Ca^{2+} variation might recruit internal stores of calcium (ER, vacuole, …) governed by receptors involved in mechanosensing, such as FERONIA or P2K1.

At the cell membrane, Ca^{2+} permeable channels activated by a force applied in the plane of the membrane were recently identified and characterized. These channels, such as RMA-DEK dependent channels or those belonging to Osca and Piezo families, behave as transducers able to convert instantaneously a mechanical force into a Ca^{2+} flux [13], [26], [44]. One might hypothesize that a pressure locally exerted on the root induces tissue strain that leads to membrane stretching. In reaction to membrane stretching, calcium permeable mechanosensitive channels will be activated. Most of these channels (RMA, Osca, Piezo) present inactivation properties, meaning that a rise of pressure applied to the membrane activates the channel, but under sustained pressure the channel enters a non-conductive state called inactivated [14]. This inactivation might, at least in part, explain the rapid (1-2 min) decrease of the Ca^{2+} signal under a long pulse of pressure delivered by the valve. In our proposed scheme, the decrease of effective response to repetitive stimulation, that we call attenuation, would be provided by a mechanical modification of cellular structural elements. An increase in the cell stiffness would limit membrane stretching and then produce less activation of calcium permeable mechanosensitive channels. Whether the cytosolic Ca^{2+} elevation plays a role in this feedback loop remains to be investigated. Even though Ca^{2+}-permeable force-gated channels

appear to be the best candidates to mediate the coupling between mechanical strain and cytosolic Ca^{2+} increase, other sensors of mechanical strains may also be involved, for example, the cytoskeleton itself, or sensors of cell wall integrity [9], [45], [46].

What could be the adaptive outcome of local calcium signaling?

A root growing in the soil squeezed between two rocks, for example, will have to locally adapt its mechanical properties by strengthening its tissues. This could be achieved through strengthening the cell wall or remodeling the cytoskeleton. The non-propagated Ca^{2+} signal locally initiated by pressure stimulation might be the event that initiates further transduction signaling cascades possibly involving pH variation, reactive oxygen species generation, and kinase activation, and further leading to developmental responses and to the root adaptation [5], [6]. In natural conditions, roots are also subjected to diurnal hydraulic pressure variations producing a periodic root diameter increase and decrease ([47]). This latter phenomenon has to be considered together with root progression in which a root squeezed in a bottleneck will be self-stimulated during growth. Root curvature additionally induces strains, and secondary roots preferentially emerge in the curved zones of the root [48]. In order to get a complete picture of strain capacity in relation with calcium variations, we will have also to explore the root elongation zone. Such an approach require the development of new microfluidic chamber.

Acknowledgements

Seeds expressing R-GECO were provided by Rainer Waadt and Melanie Krebs (Ruprecht-Karls-Universität Heidelberg, Germany). This work has benefited from a French State grant (Saclay Plant Sciences, reference n° ANR-17-EUR-0007, EUR SPS-GSR) under a France 2030 program (reference n° ANR-11-IDEX-0003) through the DYNANO project. It has also benefited from Imagerie-Gif core facility supported by l'Agence Nationale de la Recherche (ANR-11-EQPX-0029/Morphoscope, ANR-10-INBS-04/FranceBioImaging ; ANR-11-IDEX-0003-02/ Saclay Plant Sciences). We gratefully acknowledge the financial support from the Région Ile de France through the DIM ELICIT program, for the Plantuidics grant. We thank David Bouchez from IJPB (Versailles, France) for fruitful discussions and Nicolas Valentin for printing adapters to set up microfluidic chips of the microscopes.

Bibliography

[1] E. Kolb, V. Legué, and M.-B. Bogeat-Triboulot, « Physical root–soil interactions », *Physical Biology*, vol. 14, n° 6, p. 065004, nov. 2017, doi: 10.1088/1478-3975/aa90dd.

[2] J. Roué *et al.*, « Root cap size and shape influence responses to the physical strength of the growth medium in Arabidopsis thaliana primary roots », *Journal of Experimental Botany*, p. erz418, nov. 2019, doi: 10.1093/jxb/erz418.

[3] A. R. Dexter, « Advances in characterization of soil structure », *Soil and Tillage Research*, vol. 11, n° 3-4, p. 199-238, juin 1988, doi: 10.1016/0167-1987(88)90002-5.

[4] J. Bose, I. I. Pottosin, S. S. Shabala, M. G. Palmgren, and S. Shabala, « Calcium Efflux Systems in Stress Signaling and Adaptation in Plants », *Front. Plant Sci.*, vol. 2, 2011, doi: 10.3389/fpls.2011.00085.
[5] B. Ranty, D. Aldon, V. Cotelle, J.-P. Galaud, P. Thuleau, and C. Mazars, « Calcium Sensors as Key Hubs in Plant Responses to Biotic and Abiotic Stresses », *Front. Plant Sci.*, vol. 7, mars 2016, doi: 10.3389/fpls.2016.00327.
[6] W. Tian, C. Wang, Q. Gao, L. Li, and S. Luan, « Calcium spikes, waves and oscillations in plant development and biotic interactions », *Nat. Plants*, vol. 6, n° 7, p. 750-759, juin 2020, doi: 10.1038/s41477-020-0667-6.
[7] G. B. Monshausen, T. N. Bibikova, M. H. Weisenseel, and S. Gilroy, « Ca $^{2+}$ Regulates Reactive Oxygen Species Production and pH during Mechanosensing in *Arabidopsis* Roots », *Plant Cell*, vol. 21, n° 8, p. 2341-2356, août 2009, doi: 10.1105/tpc.109.068395.
[8] H. Suda *et al.*, « Calcium dynamics during trap closure visualized in transgenic Venus flytrap », *Nat. Plants*, vol. 6, n° 10, p. 1219-1224, oct. 2020, doi: 10.1038/s41477-020-00773-1.
[9] A. Voxeur and H. Höfte, « Cell wall integrity signaling in plants: "To grow or not to grow that's the question" », *Glycobiology*, vol. 26, n° 9, p. 950-960, sept. 2016, doi: 10.1093/glycob/cww029.
[10] H.-W. Shih, N. D. Miller, C. Dai, E. P. Spalding, and G. B. Monshausen, « The Receptor-like Kinase FERONIA Is Required for Mechanical Signal Transduction in Arabidopsis Seedlings », *Current Biology*, vol. 24, n° 16, p. 1887-1892, août 2014, doi: 10.1016/j.cub.2014.06.064.
[11] A.-L. Le Roux, X. Quiroga, N. Walani, M. Arroyo, and P. Roca-Cusachs, « The plasma membrane as a mechanochemical transducer », *Phil. Trans. R. Soc. B*, vol. 374, n° 1779, p. 20180221, août 2019, doi: 10.1098/rstb.2018.0221.
[12] M. Guichard, S. Thomine, and J.-M. Frachisse, « Mechanotransduction in the spotlight of mechano-sensitive channels », *Current Opinion in Plant Biology*, vol. 68, p. 102252, août 2022, doi: 10.1016/j.pbi.2022.102252.
[13] D. Tran *et al.*, « A mechanosensitive Ca2+ channel activity is dependent on the developmental regulator DEK1 », *Nat Commun*, vol. 8, n° 1, p. 1009, déc. 2017, doi: 10.1038/s41467-017-00878-w.
[14] J.-M. Frachisse, S. Thomine, and J.-M. Allain, « Calcium and plasma membrane force-gated ion channels behind development », *Current Opinion in Plant Biology*, vol. 53, p. 57-64, févr. 2020, doi: 10.1016/j.pbi.2019.10.006.
[15] R. Dangla, S. C. Kayi, and C. N. Baroud, « Droplet microfluidics driven by gradients of confinement », *Proc. Natl. Acad. Sci. U.S.A.*, vol. 110, n° 3, p. 853-858, janv. 2013, doi: 10.1073/pnas.1209186110.
[16] R. Waadt, M. Krebs, J. Kudla, and K. Schumacher, « Multiparameter imaging of calcium and abscisic acid and high-resolution quantitative calcium measurements using R-GECO1-mTurquoise in Arabidopsis », *New Phytol*, vol. 216, n° 1, p. 303-320, oct. 2017, doi: 10.1111/nph.14706.
[17] G. Grossmann *et al.*, « The RootChip: An Integrated Microfluidic Chip for Plant Science », *The Plant Cell*, vol. 23, n° 12, p. 4234-4240, déc. 2011, doi: 10.1105/tpc.111.092577.
[18] M. A. Unger, H.-P. Chou, T. Thorsen, A. Scherer, and S. R. Quake, « Monolithic Microfabricated Valves and Pumps by Multilayer Soft Lithography », *Science*, vol. 288, n° 5463, p. 113-116, avr. 2000, doi: 10.1126/science.288.5463.113.
[19] M. Meier, E. M. Lucchetta, and R. F. Ismagilov, « Chemical stimulation of the Arabidopsis thaliana root using multi-laminar flow on a microfluidic chip », *Lab Chip*, vol. 10, n° 16, p. 2147, 2010, doi: 10.1039/c004629a.
[20] L. Dupuy *et al.*, « Micromechanics of root development in soil », *Current Opinion in Genetics & Development*, vol. 51, p. 18-25, août 2018, doi: 10.1016/j.gde.2018.03.007.
[21] A. M. Abdalla, D. R. P. Hettiaratchi, and A. R. Reece, « The mechanics of root growth in Granular media », *Journal of Agricultural Engineering Research*, vol. 14, n° 3, p. 236-248, sept. 1969, doi: 10.1016/0021-8634(69)90126-7.

[22] W. K. Silkand K. K. Wagner, « Growth-sustaining Water Potential Distributions in the Primary Corn Root: A NONCOMPARTMENTED CONTINUUM MODEL », *Plant Physiol.*, vol. 66, n° 5, p. 859-863, nov. 1980, doi: 10.1104/pp.66.5.859.
[23] E. Kolb, C. Hartmann,and P. Genet, « Radial force development during root growth measured by photoelasticity », *Plant Soil*, vol. 360, n° 1-2, p. 19-35, nov. 2012, doi: 10.1007/s11104-012-1316-2.
[24] V. Mirabet, P. Das, A. Boudaoud, and O. Hamant, « The Role of Mechanical Forces in Plant Morphogenesis », *Annu. Rev. Plant Biol.*, vol. 62, n° 1, p. 365-385, juin 2011, doi: 10.1146/annurev-arplant-042110-103852.
[25] A. Geitmann, « Experimental approaches used to quantify physical parameters at cellular and subcellular levels », *American J of Botany*, vol. 93, n° 10, p. 1380-1390, oct. 2006, doi: 10.3732/ajb.93.10.1380.
[26] S. A. R. Mousavi *et al.*, « PIEZO ion channel is required for root mechanotransduction in *Arabidopsis thaliana* », *Proceedings of the National Academy of Sciences*, vol. 118, n° 20, p. e2102188118, mai 2021, doi: 10.1073/pnas.2102188118.
[27] E. Matthus *et al.*, « DORN1/P2K1 and purino-calcium signalling in plants: making waves with extracellular ATP », *Annals of Botany*, vol. 124, n° 7, p. 1227-1242, déc. 2019, doi: 10.1093/aob/mcz135.
[28] J. Choi *et al.*, « Identification of a plant receptor for extracellular ATP. », *Science (New York, N.Y.)*, vol. 343, n° 6168, p. 290-4, janv. 2014, doi: 10.1126/science.343.6168.290.
[29] C. T. Nguyen, A. Kurenda, S. Stolz, A. Chételat, and E. E. Farmer, « Identification of cell populations necessary for leaf-to-leaf electrical signaling in a wounded plant », *Proc. Natl. Acad. Sci. U.S.A.*, vol. 115, n° 40, p. 10178-10183, oct. 2018, doi: 10.1073/pnas.1807049115.
[30] H. Knight, A. J. Trewavas, and M. R. Knight, « Cold calcium signaling in Arabidopsis involves two cellular pools and a change in calcium signature after acclimation. », *Plant Cell*, vol. 8, n° 3, p. 489-503, mars 1996, doi: 10.1105/tpc.8.3.489.
[31] G. J. Allen *et al.*, « A defined range of guard cell calcium oscillation parameters encodes stomatal movements », *Nature*, vol. 411, n° 6841, p. 1053-1057, juin 2001, doi: 10.1038/35082575.
[32] L. Martin, N. Leblanc-Fournier, J.-L. Julien, B. Moulia, and C. Coutand, « Acclimation kinetics of physiological and molecular responses of plants to multiple mechanical loadings », *Journal of Experimental Botany*, vol. 61, n° 9, p. 2403-2412, mai 2010, doi: 10.1093/jxb/erq069.
[33] F. Kramer *et al.*, « Inhibitory glycinergic neurotransmission in the mammalian auditory brainstem upon prolonged stimulation: short-term plasticity and synaptic reliability », *Front. Neural Circuits*, vol. 8, mars 2014, doi: 10.3389/fncir.2014.00014.
[34] E. Friauf, A. U. Fischer, and M. F. Fuhr, « Synaptic plasticity in the auditory system: a review », *Cell Tissue Res*, vol. 361, n° 1, p. 177-213, juill. 2015, doi: 10.1007/s00441-015-2176-x.
[35] L. Yue, J. Feng, R. Gaspo, G.-R. Li, Z. Wang, and S. Nattel, « Ionic Remodeling Underlying Action Potential Changes in a Canine Model of Atrial Fibrillation », *Circulation Research*, vol. 81, n° 4, p. 512-525, oct. 1997, doi: 10.1161/01.RES.81.4.512.
[36] S. M. Cain and T. P. Snutch, « Contributions of T-type calcium channel isoforms to neuronal firing », *Channels*, vol. 4, n° 6, p. 475-482, nov. 2010, doi: 10.4161/chan.4.6.14106.
[37] A. H. Howell *et al.*, « Pavement cells distinguish touch from letting go », *Nat. Plants*, mai 2023, doi: 10.1038/s41477-023-01418-9.
[38] B. Gardiner, P. Berry, and B. Moulia, « Review: Wind impacts on plant growth, mechanics and damage », *Plant Science*, vol. 245, p. 94-118, avr. 2016, doi: 10.1016/j.plantsci.2016.01.006.
[39] A. Sampathkumar *et al.*, « Subcellular and supracellular mechanical stress prescribes cytoskeleton behavior in Arabidopsis cotyledon pavement cells », *eLife*, vol. 3, p. e01967, avr. 2014, doi: 10.7554/eLife.01967.
[40] K. R. James, J. R. Moore, D. Slater, and G. A. Dahle, « Tree biomechanics. », *CABI Reviews*, vol. 2017, p. 1-11, janv. 2017, doi: 10.1079/PAVSNNR201712038.

[41] B. Moulia, C. Coutand, and J.-L. Julien, « Mechanosensitive control of plant growth: bearing the load, sensing, transducing, and responding », *Front. Plant Sci.*, vol. 6, févr. 2015, doi: 10.3389/fpls.2015.00052.
[42] T. A. DeFalco, K. W. Bender, and W. A. Snedden, « Breaking the code: Ca2+ sensors in plant signalling », *Biochemical Journal*, vol. 425, n° 1, p. 27-40, janv. 2010, doi: 10.1042/BJ20091147.
[43] F. Resentini *et al.*, « Simultaneous imaging of ER and cytosolic Ca2+ dynamics reveals long-distance ER Ca2+ waves in plants », *Plant Physiology*, vol. 187, n° 2, p. 603-617, oct. 2021, doi: 10.1093/plphys/kiab251.
[44] S. E. Murthy *et al.*, « OSCA/TMEM63 are an evolutionarily conserved family of mechanically activated ion channels », *eLife*, p. 17, 2018.
[45] O. Hamant, D. Inoue, D. Bouchez, J. Dumais, and E. Mjolsness, « Are microtubules tension sensors? », *Nat Commun*, vol. 10, n° 1, p. 2360, mai 2019, doi: 10.1038/s41467-019-10207-y.
[46] A. Fruleux, S. Verger, and A. Boudaoud, « Feeling Stressed or Strained? A Biophysical Model for Cell Wall Mechanosensing in Plants », *Front. Plant Sci.*, vol. 10, p. 757, juin 2019, doi: 10.3389/fpls.2019.00757.
[47] T. Henzler *et al.*, « Diurnal variations in hydraulic conductivity and root pressure can be correlated with the expression of putative aquaporins in the roots of Lotus japonicus », *Planta*, vol. 210, n° 1, p. 50-60, nov. 1999, doi: 10.1007/s004250050653.
[48] G. L. Richter, G. B. Monshausen, A. Krol, and S. Gilroy, « Mechanical Stimuli Modulate Lateral Root Organogenesis », *Plant Physiol.*, vol. 151, n° 4, p. 1855-1866, déc. 2009, doi: 10.1104/pp.109.142448.

Supplementary data

Local compression of the root in a microfluidic device triggers a calcium signal

Vassanti Audemar, Yannick Guerringue, Joni Frederick, Pauline Vinet, Isaty Melogno, , Avin Babataheri, Valérie Legué, Sébastien Thomine, Jean-Marie Frachisse

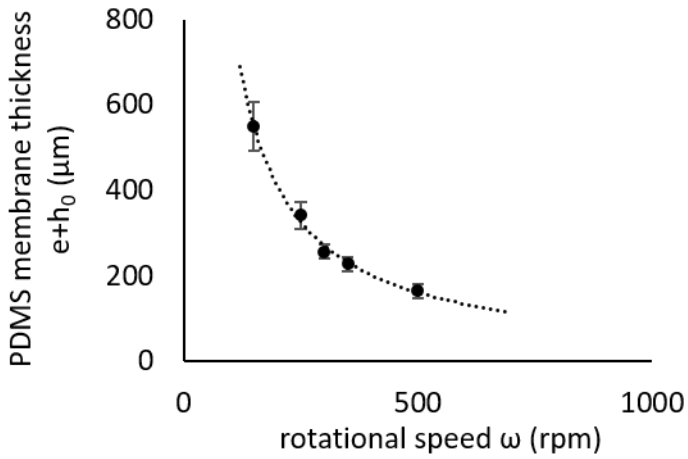

S-Fig 1: PDMS membrane thickness variations with ω, the rotational speed during the spin coating process. Circles correspond to experimental data and the dotted line corresponds to the power law fit given by the equation $(e+h_0) = 0.09\omega^{-1,02}$. The fit of the curve with a power law is in agreement with Koschwanez et al. [49] and Zhang et al. [50].

[49] J. H. Koschwanez, R. H. Carlson, and D. R. Meldrum, « Thin PDMS Films Using Long Spin Times or Tert-Butyl Alcohol as a Solvent », *PLoS ONE*, vol. 4, n° 2, p. e4572, févr. 2009, doi: 10.1371/journal.pone.0004572.

[50] W. Y. Zhang, G. S. Ferguson, and S. Tatic-Lucic, « Elastomer-supported cold welding for room temperature wafer-level bonding », in *17th IEEE International Conference on Micro Electro Mechanical Systems. Maastricht MEMS 2004 Technical Digest*, Maastricht, Netherlands: IEEE, 2004, p. 741-744. doi: 10.1109/MEMS.2004.1290691.

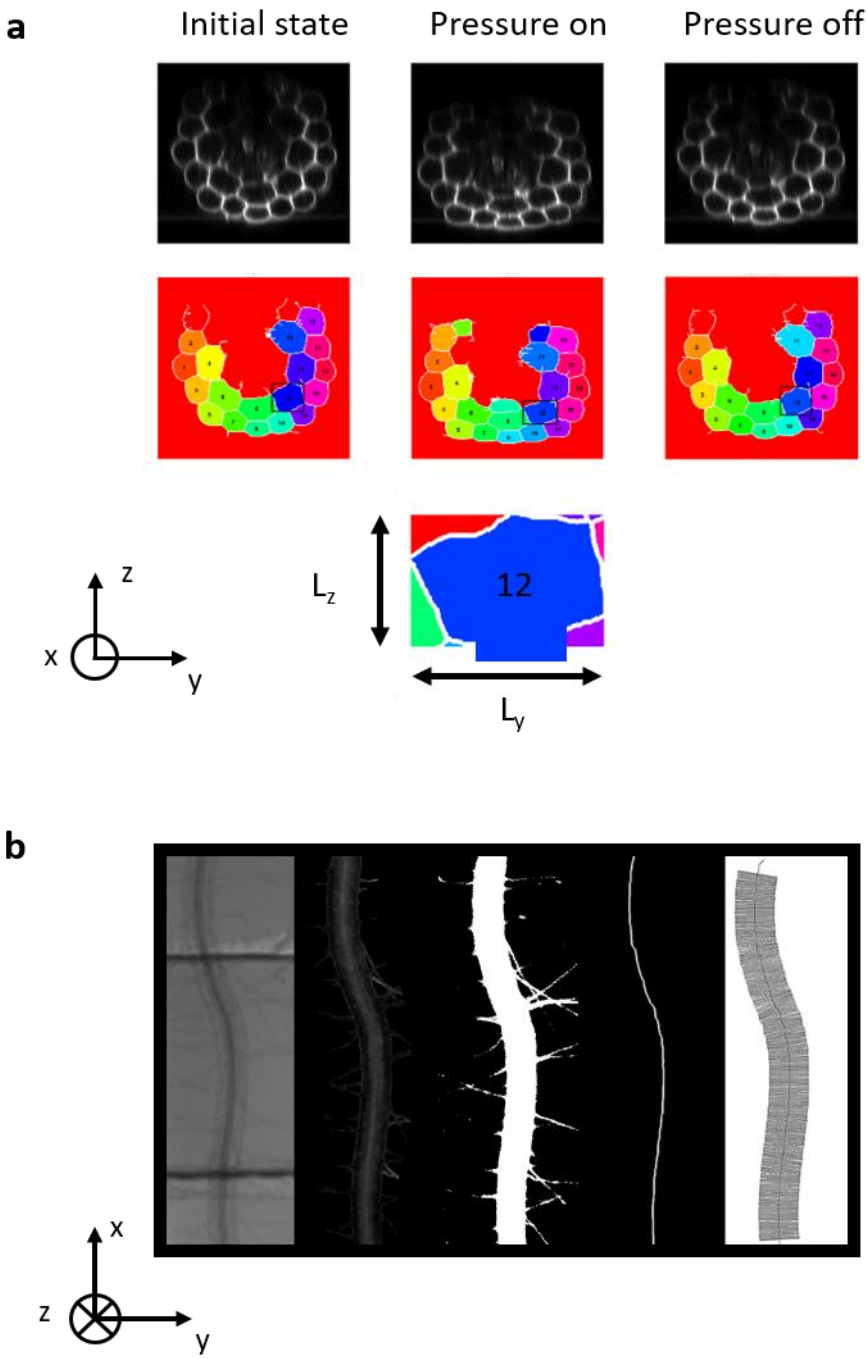

S-Fig. 2: Image analysis procedure: a) Cross-sectional image of the root cells at rest, under a lateral pressure of 90 kPa and after release of the pressure; Top images (black and white), fluorescent images with cell walls colored with propidium iodide (5 µg/mL) and imaged with λexc = 488 nm and λem = 551-651 nm, Middle images (colored), segmented cells separated with white lines, colors have no other purpose than differentiating cells between each other. Cell number 12 is framed by a black bounding box and represented in the bottom line. The maximum height L_z and the maximum width L_y of the cell are indicated. b) Top view image of the root under the valve (from left to right) : bright field image, mTurquoise fluorescent image (λexc = 470 nm and λem = 490-520 nm), binarized image, and skeletonized axis of the root, segments (100 µm length) perpendicular to the root axis and distributed every 50 pixels.

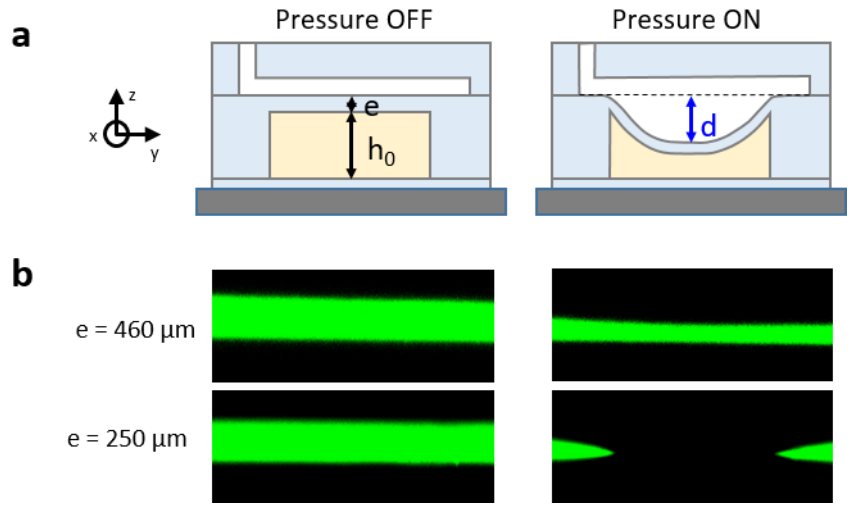

S-Fig 3: a) Schematic cross section of the PDMS device showing deformation of the pneumatic valve with and without pressure: e is the thickness of the PDMS membrane separating pressure channel (in white) and the root channel (in yellow), h0 is the thickness of the root channel without pressure and is equal to 90 µm, d is the maximum distance between the center of the valve membrane at rest and in its deformed state. b) Cross-sectional view of the microfluidics channels filled with a dilute solution of fluorescein without (left) and with (right) 75 kPa of pressure for two different PDMS membrane thicknesses: e = 460 µm (top image), e= 250 µm (bottom image). Deformability of the PDMS membrane decreases with its thickness.

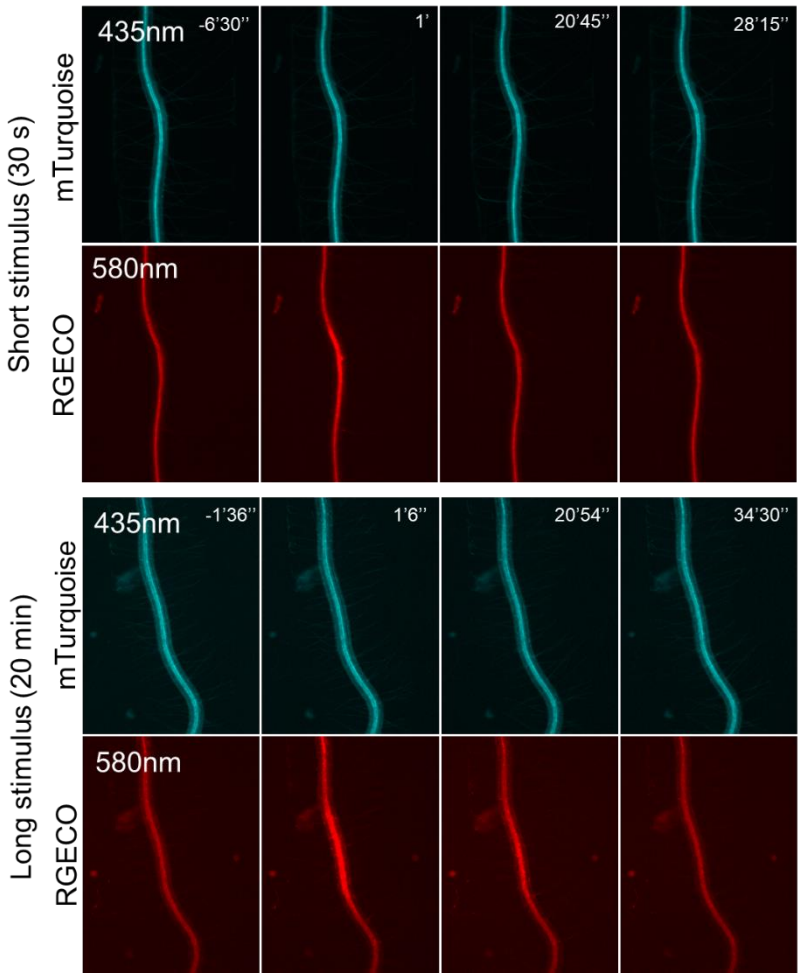

S-Fig. 4: RGECO and mTurquoise fluorescence frames taken at different times before or after the activation and release of pressure. The origin of time is set at the activation of pressure. These frames were used to calculate the ratio frames showed in Fig 4, for a short stimulus of 30s and a long stimulus of 20 min.

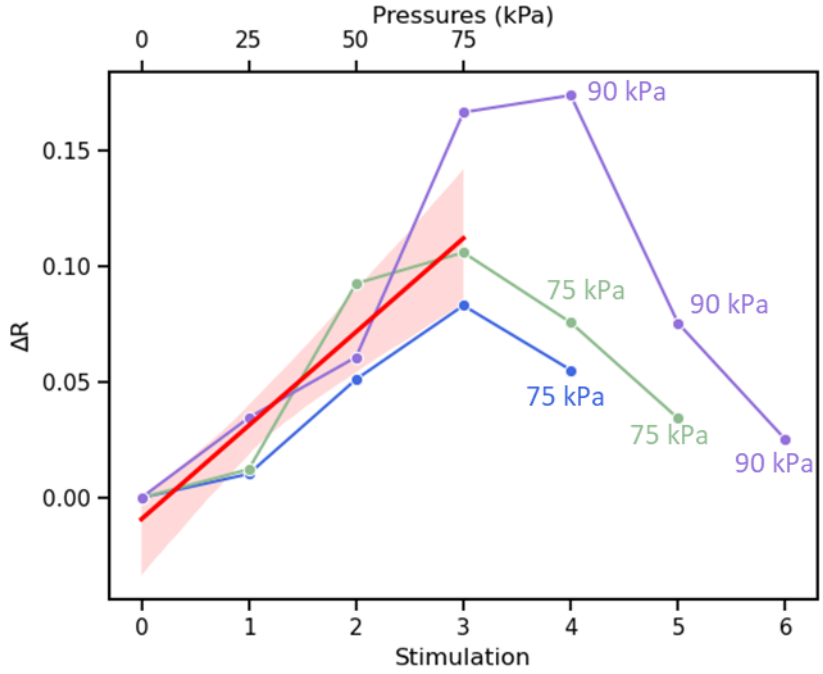

S-Fig 5: Successive stimulations of 30 s with an increasing pressure. Amplitude of the calcium signal for each stimulation in three different roots represented in blue, green and purple disks., Stimulations 4 to 6: pressure as indicated on the graph. The red line correspondsStimulations 1 to 3 are the one of Fig. 5a to the linear regression on stimulations 1 to 3 plotted with a confidence interval (band) (slope = , R^2 = 0.90, p-value = $7x10^{-5}$).

SUPPLEMENTARY VIDEO 1

Deformation of the root stimulated 6 times every 5 min with a pressure of 90 kPa during 1 min. Cross-sectional video of the root with cell walls colored with propidium iodide (5 µg/mL) and imaged with λexc = 488 nm and λem = 551-651 nm. The pressure is applied from the top and the playing speed is accelerated 50 times

SUPPLEMENTARY VIDEO 2

Calcium response of the root to a local pressure of 90 kPa applied during 30 sec (short stimulation). Variations of the normalized ratio RGECO1-mTurquoise fluorescence (λexc and λem of RGECO1 and mTurquoise, see Material and Method).The red line correspond to the position of the pneumatic valve. The playing speed is accelerated 100 times

SUPPLEMENTARY VIDEO 3

Calcium response of the root to a local pressure of 90 kPa applied during 20 min (long stimulation). Variations of the normalized ratio RGECO1-mTurquoise fluorescence (λexc and λem of RGECO1 and

mTurquoise, see Material and Method).The red line correspond to the position of the pneumatic valve. The playing speed is accelerated 100 times